A PLANAR PARALLEL MANIPULATOR WITH HOLONOMIC HIGHER PAIRS: INVERSE KINEMATICS

Matthew John D. HAYES [1] *Paul J. ZSOMBOR–MURRAY* [2]

[1,2] McGill University, Centre for Intelligent Machines, Department of Mechanical Engineering
817 r. Sherbrooke O., Rm 454, Montréal, Québec, H3A 2K6 Canada, Tel: (514) 398–6311
Fax: (514) 398–4476, email: <johnh@cim.mcgill.ca>, <paul@cim.mcgill.ca>

ABSTRACT

Pure rolling between bodies in contact, as is sometimes used for fine–motion manipulation, is an important research issue. Furthermore, inverse kinematic (IK) solutions are necessary to plan trajectories and avoid obstacles. In this paper, closed form analytical solutions to the IK problem of a 3–degree–of–freedom (DOF) planar parallel manipulator with holonomic higher pairs are presented. This manipulator is a single closed loop kinematic chain whose end–effector is a circular disk which rolls without slip along a straight line on the non–grounded rigid links of each of two 2R serial legs. The points of contact between the disk and the legs constitute holonomic higher pairs. The pairs are termed 'holonomic' because the constraint equations are in integral form. The solution algorithm is novel because the holonomic constraint equations and the axiom of *closure* pertaining to the group of isometries of the plane are exploited. It is shown that any general plane motion of the disk within the physical limits of the workspace is decomposable into a single pure translation of the disk and a single rotation of the disk about its centre. Furthermore, these specific translations and rotations commute. Five special properties of the manipulator allow a set of intermediate joint variables, calculated for pure translation, to be combined with a subsequent set for pure rotation, given the desired and initial pose of the disk. Since the solutions for the joint variables of each leg are uncoupled, the solution algorithm is generalized such that joint variables can be determined for rolling systems containing 2R legs of any number, n. There are no more than 4^n real IK solutions. Three illustrative examples are given.

1. INTRODUCTION

Extensive recent research has been done in connection with grasping and fine–motion manipulation by multi-fingered robotic hands, [13]. The Utah/MIT dextrous hand is an example. Various types of contact between finger and hand have been studied extensively in [17]. The kinematics of rolling contact for two surfaces of arbitrary shape was examined in [6]. Control schemes for parallel manipulators with rolling constraints were put forward in [19, 6]. Rolling is found elsewhere, *e.g.*, automatically guided vehicles (AGV) are used industrially to convey cargo. The kinematics and dynamics of a three wheeled 2 DOF AGV were studied in great detail in [15].

Robotic mechanical systems involving rolling contact rarely use higher pair joints. For instance, most robotic hands are constructed with lower pairs only and the rolling contact is between end–effector and workpiece, [17]. In the case of the AGV, continuous rolling contact is a by–product of constraints imposed by the operating environment. It is not a design parameter affecting control (except to detect wheel slip) or kinematic synthesis.

With the exception of cams and gears, which are not considered to be robotic mechanical devices, research on mechanisms containing higher pairs is rare. The rolling–without–slipping pair is considered here in this regard because gearing is common, efficient and reliable but uncommon in robotic manipulators.

If the rolling is restricted to a one parameter planar motion, the rolling constraints are holonomic because the constraint equations can be expressed in terms of displacement, i.e., in integral form, thereby simplifying kinematic analysis. Very little literature on such planar mechanisms was found. The effects of initial assembly configurations on the reachable workspace of a planar rolling system were examined in [3]. Previously the same authors, [2], described an algorithm for the inverse kinematics (IK) problem of the same manipulator. However, they failed to account for the orientation of the end–effector in the inertial reference frame. That is, a relative angle, used to specify orientation, can change while the orientation of the end effector remains constant and so erroneous solutions arise. We found no other reference to the IK problem of such a planar manipulator.

Optimal trajectory planning and obstacle avoidance in a crowded workspace requires fast computation of IK solutions. Hence, with this in mind, the objective of this paper is to investigate the IK problem of a 3–DOF planar parallel manipulator with holonomic higher pairs. We show that, when some concepts from elementary planar Euclidean geometry are employed, "trivial", closed form solutions are obtained. Throughout, we emphasize "geometric thinking", ideas raised in [20], to formulate an IK solution, while its triviality was revealed in [10].

In the next section the manipulator is described. Section 3 gives a detailed description of the nomenclature required for the generalization of the analysis to manipulators of n 2R legs. The fourth section lists five special properties observed from the kinematic geometry of the manipulator germane to the IK algorithm. Section 5 discusses disk motions in the plane and decompositions of general displacements. Section 6 describes the four step solution algorithm. In section 7 closed form analytic solutions to the inverse kinematics problem are presented. Three examples are given in section 8 and an appendix contains their tabulated results.

2. MANIPULATOR DESCRIPTION

A single closed loop manipulator is shown in Fig. 1. It consists of 5 articulated links, which move with

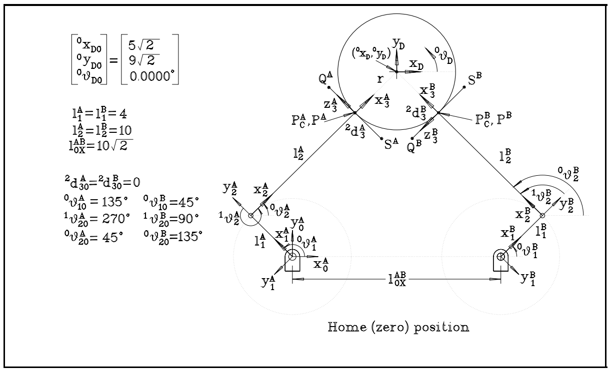

Figure 1. A planar parallel manipulator with two holonomic higher pairs.

constrained relative motion, and a grounded base. These six members are connected by 4 revolute (R) joints (lower pairs) and 2 points of pure rolling contact (higher pairs). The end–effector, disk D, is the link -G-G- in the -R-R-G-G-R-R- loop. Legs A and B each consist of two links. The first link in each leg is grounded to the base, connected by an R–pair and to the second link by another R–pair. The disk rolls, without slip, over the surface of the straight lines $Q^A S^A$ and $Q^B S^B$ which are perpendicular to l_2^A and l_2^B of the serial legs A and B. These lines are constrained to remain in tangential contact with the disk, although the points of tangency are varied by relative rolling of the lines with respect to the disk. The points of contact P_C^A and P_C^B between the disk and legs constitute two holonomic higher kinematic pairs.

The inverse kinematics problem involves the determination of a set of feasible joint variables required to attain a desired disk pose. The algebra is simplified by expressing each joint variable in its own reference frame. Variables in the cascaded reference frames are transformed to other reference frames as the problem requires. Careful selection of frame origins will simplify computation. Hence, link reference frames are assigned using the well established procedure developed by Denavit and Hartenberg [9, 11] and adapted for higher pairs here. The procedure is summarized below:

1. Identify the point of intersection, or the common normal of neighbouring joint axes i and $i+1$. Assign the origin of the frame for link i at the point of intersection, or where the common normal meets the i^{th} axis.
2. Assign the z_i direction pointing along the i^{th} joint axis.
3. Assign the x_i direction pointing along the common normal, or if the axes intersect, assign x_i to be normal to the plane containing the two axes.
4. Assign the y_i direction to complete a right–handed coordinate system.

This procedure introduces the planar systems $x-y$ and $y-z$. These systems are used for their computational convenience when concatenating the 4×4 DH parameter transformations, mentioned later on, to derive the displacement equations. Fig. 1 shows the manipulator with link frames assigned this way.

3. NOMENCLATURE

The kinematic analysis of a parallel manipulator is the same as that for a serial manipulator, except that the solution is repeated for each leg, [10]. So joint and position variables along with link design parameters must be generalized to allow for analysis of the manipulator on a leg by leg basis. To minimize the confusion that results from the handling of the kinematic relationships in component form, a well defined, unambiguous notation must be adopted. Therefore, each joint and position variable is fully identified by left and right sub and super–scripts while link parameters require only right sub and super–scripts as described below.

i) Left and right sub and super–scripts.

1. For a joint variable, the right sub–script i, $i \in \{1, 2, 3\}$ identifies the joint number. For each manipulator leg, the joint number at the connection between the first link and the base is 1. Between the first and second links is 2. The higher pair between link 2 and the disk is 3.
2. For a coordinate axis, the right sub–script i, $i \in \{0, 1, 2, \ldots, i\}$ represents the link to which the coordinate system is attached. 0 is for the base, 1 is for the first link, etc..
3. The right super–script, j, $j \in \{A, B, \ldots, j\}$ denotes a particular manipulator leg.
4. The left super–script, f, $f \in \{0, 1, 2 \ldots, f\}$ refers to the reference frame in which the variable is represented.
5. The left sub–script, m indicates the type of planar motion. R is for pure rotation of the disk about its centroid. T is for pure translation of the disk centre. No left sub–script means either general plane motion, or that the type of motion is obvious from the context.

ii) Fixed link design parameters.

1. l_i^j is the length of link i in leg j.
2. l_{0x}^{jk} is the projected distance along the horizontal axis of the inertial reference frame, $\{{}^A_0\}$ between the origins of legs j and k, $j \in \{A, B, \ldots, j\}$, $k \in \{A, B, \ldots, k\}$, $j \neq k$. Note: For all analysis in this paper the base frame $\{{}^A_0\}$ of leg A is considered as the inertial reference frame.
3. l_{0y}^{jk} is the projected distance along the vertical axis of the inertial reference frame, $\{{}^A_0\}$ between the origins of legs j and k, $j \in \{A, B, \ldots, j\}$, $k \in \{A, B, \ldots, k\}$, $j \neq k$.
4. r is the radius of the disk.

iii) Joint variables.

1. ${}^f_m\vartheta_i^j$ is the joint angle i of leg j described in reference frame f with regard to m type of motion. Positive angles are measured counter–clockwise (CCW).
2. ${}^2_m d_3^j$ is the distance from point P^j to point P_C^j measured along y_2^j. Note that y_2^j and z_3^j are always parallel. So d_3^j could be measured in frame $\{{}^j_3\}$ along z_3^j. However, in order to later derive the manipulator displacement equations using DH parameters, d_3^j must be expressed in frame $\{{}^j_2\}$.
In the home position shown in Fig. 1, the points P^j and P_C^j are coincident. The origin of the frame $\{{}^j_3\}$ is superimposed on the point of contact between the straight line $Q^j S^j$, and the disk D, and translates with it along line $Q^j S^j$.

iv) Position variables: The Pose Array.

The *pose* of the disk will be described by a 3×1 array composed of the following variables, all expressed in the inertial reference frame:

$$\begin{bmatrix} x_D \\ y_D \\ \vartheta_D \end{bmatrix}$$

Where

1. x_D is the x cartesian coordinate of the disk centre.
2. y_D is the y cartesian coordinate of the disk centre.
3. ϑ_D is the orientation of the disk expressed as the angle between the x_D axis and the x_0^A axis. In the home position, the x_D axis is parallel to the x_0^A axis.

4. SPECIAL MANIPULATOR PROPERTIES

The general motion of the disk in the plane involves relative motion between the disk and each serial 2R leg. The rolling contact is conveniently modelled as multiple racks and a single pinion. Each rack can roll on the pinion, the pinion can roll on the racks, or there can be a combination of the two motions. For general planar motion the system, with link frames as assigned in Fig. 1, has the following properties which, for the sake of brevity, are stated without proof:

1. If the pinion rolls on one rack, then it must roll on both.
2. Either or both racks may roll on the pinion.
3. If, during general motion, the pinion is stationary with respect to one rack while the other rack rolls on the pinion there are two possibilities. First, let's suppose the higher pair in the A leg is locked. If ${}^0\vartheta_2^A$ is constant the motion of the pinion is pure curvilinear translation in the fixed base frame. Second, if ${}^0\vartheta_2^A$ changes during the motion, then the pinion rotates about a centre other than its own axis by an angle equal to the change in ${}^0\vartheta_2^A$.
4. If $\Delta^2 d_3^A$ has the same magnitude but opposite sense as $\Delta^2 d_3^B$, then the motion of the pinion is pure rectilinear translation of its centre. Pure curvilinear translation can also occur if the magnitude condition is violated however, the opposite sense condition must be met.
5. If $\Delta^2 d_3^A$ and $\Delta^2 d_3^B$ have the same magnitude and sense, then the motion of the pinion is pure fixed axis rotation about its centre.

These properties may be extended to manipulators with more than two legs by replacing the words 'both' & 'either' with 'all' & 'any'.

5. DISK MOTIONS IN THE PLANE

An Isometry of the Euclidean Plane is a one–to–one mapping of the plane onto itself which leaves distance invariant [7]. The set of all planar isometries belong to an algebraic group. A group consists of a set, $\mathcal{G}$ together with a binary operator, $*$ defined on $\mathcal{G}$ which satisfies the following axioms, [4]:

1) $x * y \in \mathcal{G}$	$\forall\ x, y \in \mathcal{G}$
2) $(x * y) * z = x * (y * z)$	$\forall\ x, y, z \in \mathcal{G}$
3) $\exists\ I \in \mathcal{G}$:	$I * x = x * I = x$, $\forall\ x \in \mathcal{G}$
4) $\exists\ x^{-1} \in \mathcal{G}$:	$x * x^{-1} = x^{-1} * x = I$, $\forall\ x \in \mathcal{G}$

1) through 4) are known as the *closure, associativity, identity,* and *inverse* axioms, respectively. Note that commutativity is not a group axiom.

A planar displacement consists of the direct isometries only. The direct isometries are translations and rotations. Since direct isometries preserve sense as well as distance, the product of any number of direct isometries is another direct isometry. It is easy to show that the associativity axiom holds for the product of three direct isometries. It is equally simple to show the existence of an identity displacement and that there is an inverse for every displacement in the plane. Hence, the set of all planar displacements is a sub–group of the group of isometries of the plane. Note that the indirect, or opposite isometries do not preserve sense and therefore do not form a sub–group since the product of opposite isometries is not necessarily opposite.

Let $\mathcal{D}$ be the sub–group of planar displacements. The manipulator under study has 3 DOF. Two are translations in the x_0^A and y_0^A directions, and one rotation about the centre of the disk. The group operator in $\mathcal{D}$, $*$, called "product", represents successive implementations of given isometries. By virtue of the axiom of *closure*, all the products of all translations and all rotations are also in $\mathcal{D}$. Hence, The disk can move in any combination of translation and rotation within the physical limitations of its workspace.

It is well established, and quite simple to show that any displacement of the disk, that is, any product of translations and rotations about arbitrary parallel axes normal to the plane may be decomposed into the product of a single translation of the disk centre and a single rotation through a finite angle of the disk about its centre. Furthermore, since it is the centre of rotation which is translated, these specific translations and rotations commute. The latter claim is shown by the following: Let

$$\begin{aligned} \mathcal{T}_d &= \text{Translation through distance } d. \\ \mathcal{S}_\Phi &= \text{Rotation through angle } \Phi \text{ about centre } S. \end{aligned}$$

Consider the arbitrary motion of the disk along some path between an initial position, P_i, and a final position P_f shown in Fig. 2. $\mathcal{T}_d$ is the translation through

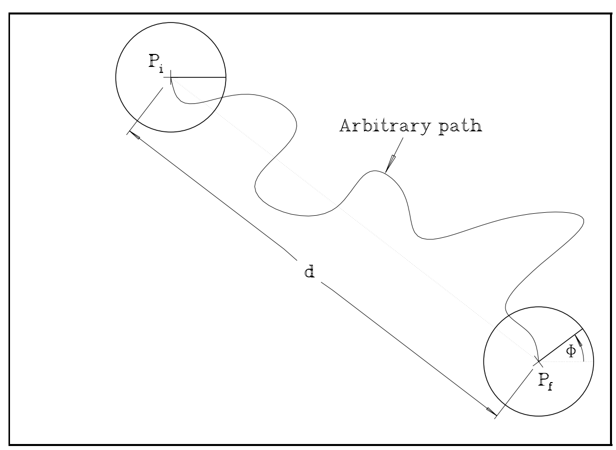

Figure 2. Arbitrary motion of the disk between two points.

distance d of the disk centre from P_i to P_f. The distance d, evidently, is independent of the path between the two points. In fact, d is the sum of the directed displacements along *any* path between P_i and P_f.

Along any arbitrary path, the disk orientation can change such that when it arrives at P_f, a reference line painted on the disk has been displaced through an angle Φ. This angle is the sum of all angular displacements of the disk about arbitrary parallel axes (perpendicular to the plane of the disk) encountered along the path. Evidently, the sum may be expressed as the difference between Φ_f and Φ_i, such that $\Phi_f \equiv \Phi_i (\mathrm{mod} 2\pi)$. It follows that the sum of all angular displacements along the path may be expressed as a single rotation of the disk about its centre, $\mathcal{S}_\Phi$, where $\Phi = \Phi_f - \Phi_i$.

Apparently then, any arbitrary motion of the disk may be represented by a single translation of its centre and a single rotation about its centre. The centre of the disk is a point. Points can not rotate, they can only translate. Since the centre of rotation is translated it is evident that $\mathcal{S}_\Phi$ may occur independently from $\mathcal{T}_d$. It then follows that:

$$\mathcal{T}_d * \mathcal{S}_\Phi \quad = \quad \mathcal{S}_\Phi * \mathcal{T}_d$$

It may then be said that $\mathcal{T}_d$ and $\mathcal{S}_\Phi$ commute for decompositions of this type.

6. INVERSE KINEMATICS ALGORITHM

The problem at hand is, given $[x_D, y_D, \vartheta_D]^T$ determine $[{}^0\vartheta_1^j, {}^1\vartheta_2^j, {}^2d_3^j]^T$. A complicating factor in general plane displacement is the ambiguity that the rolling constraint introduces. That is, ϑ_D, the desired final disk orientation does not divulge how much of the new position was achieved by rotation of links 1 and 2 and how much was achieved by pure rolling between the disk and the legs. By how much has the disk rolled on the racks and by how much has each rack rolled on the disk? Is there a combination, and if so, what is the ratio? These questions lead to difficulties in the calculation of the joint offsets ${}^2d_3^j$. To address these problems the special properties of the manipulator and the group properties of $\mathcal{D}$ are invoked. Any feasible general displacement of the disk can then be decomposed into a pure translation of the disk and pure, fixed axis rotation about the centre of the disk.

Given both the desired pose array and the initial conditions, a set of intermediate joint variables may be calculated for the pure translation component. The translation set may then be combined with a subsequent set calculated for the pure rotation component. As shown earlier, these rotations and translations commute. Hence, the order of rotation and translation is not important. This last fact will be used for the sake of convention: The intermediate solutions for pure translation will be calculated first. Then, using this intermediate set as new initial conditions, solutions will be generated for fixed axis rotation. The final solution set is simply the combination of the two solution sets.

Since the solutions for each leg are not coupled, [10], each leg is treated as an open four–bar chain and solved for separately. Another convention, mentioned earlier, is that the inertial reference frame will remain coincident with the fixed reference frame of leg A. The choice of leg A is arbitrary however, any subsequent legs will be labelled $B, C, \ldots, j$, CCW from leg A. Leg A will always be solved for first. The inverse kinematics algorithm is summarized in the following four steps.

Step 1. Pure translation: Remove the higher pair connection with all but the leg being considered. The first iteration concerns leg A. Lock the higher pair so that $\Delta^2 d_3^A = 0$ and calculate the joint angles required to reach the new position given by the ordered pair (x_D, y_D). Call the new angles ${}^0_T\vartheta^A_{10}$, ${}^1_T\vartheta^A_{20}$ and ${}^0_T\vartheta^A_{20}$ (recall that ${}^0_T\vartheta^A_{20} = {}^0_T\vartheta^A_{10} + {}^1_T\vartheta^A_{20}$)

Step 2. Remove artificial angular offset: Recall special property 3): If the disk is stationary with respect to one rack while in motion, then the disk orientation can change. Since pure translation of the disk is required, any angular offset created by step 1 must be removed. This is accomplished by an imaginary fixed axis rotation about the disk centre equal in magnitude, but opposite in sense to ${}^0_T\vartheta^A_{20}$. Calculate ${}^2_Td^A_3$, which is the joint offset required to effect the imaginary rotation. Recalculate the joint angles. These are the joint angles necessary to cause the pure translation of the disk centre. Call these intermediate angles ${}^0_T\vartheta^A_1$, ${}^1_T\vartheta^A_2$ and ${}^0_T\vartheta^A_2$. Of course, if there is no rotation component to the motion, these are the final joint angles. If there is no translation component, these angles are the same as the initial joint angles.

Step 3. Pure rotation: Recall special property 5): If $\Delta^2 d_3^A$ and $\Delta^2 d_3^B$ have the same magnitude and sense, then the motion of the disk is pure rotation about its centre. Hence, $\Delta^2 d_3^A$ is simply calculated from the arc length subtended by ϑ_D, and is the same for all legs. Using the joint variables from step 2 as initial conditions and the desired disk angle ϑ_D, calculate ${}^0\vartheta_1^A$, ${}^1\vartheta_2^A$, and ${}^2d_3^A$

Step 4. Repeat Steps 1, 2, and 3 for the remaining legs.

7. CLOSED FORM ANALYTIC SOLUTION

The displacement equations for the two–legged version of the manipulator are readily obtained by inspection. But, as the number of legs and kinematic loops grows determining these equations becomes more difficult and the utility of the DH notation becomes evident. After assigning link reference frames by the procedure given in section 2, the following definitions of link parameters apply [8, 9]:

$$\begin{aligned} a_i &= \text{distance from } z_i \text{ to } z_{i+1} \text{ along } x_i. \\ \alpha_i &= \text{angle between } z_i \ \&\ z_{i+1} \text{ about } x_i. \\ d_i &= \text{distance from } x_{i-1} \text{ to } x_i \text{ along } z_i. \\ \vartheta_i &= \text{angle between } x_{i-1} \ \&\ x_i \text{ about } z_i. \end{aligned}$$

Using homogeneous Cartesian coordinates [18] with a homogenizing coordinate of $w = 1$, the relative displacement between adjacent links can be expressed as a linear transformation of the form:

$${}^{i+1}\mathbf{x} \quad = \quad {}^{i+1}_{i}\mathbf{T}\,{}^i\mathbf{x}$$

Where ${}^{i+1}\mathbf{x}$ and ${}^i\mathbf{x}$ are the position vectors of points in reference frames $\{i+1\}$ and $\{i\}$ respectively with $\mathbf{x}$ having the form:

$$\begin{bmatrix} x \\ y \\ z \\ 1 \end{bmatrix}$$

Where either y or z will be set to zero, depending on which reference plane is used (see Fig. 1). The third dimension is included for the sake of computation and has no effect on the outcome. The operator ${}^{i+1}_{i}\mathbf{T}$ is a 4×4 transformation matrix which maps vectors defined in frame i into frame $i+1$. Employing the DH parameters, it has the form:

$$ {}^{i+1}_{i}T = \begin{bmatrix} c\vartheta_i & -s\vartheta_i & 0 & a_{i-1} \\ s\vartheta_i c\alpha_{i-1} & c\vartheta_i c\alpha_{i-1} & -s\alpha_{i-1} & -s\alpha_{i-1}d_i \\ s\vartheta_i s\alpha_{i-1} & c\vartheta_i s\alpha_{i-1} & c\alpha_{i-1} & c\alpha_{i-1}d_i \\ 0 & 0 & 0 & 1 \end{bmatrix} $$

Where $c \equiv \cos$ and $s \equiv \sin$.

A transformation matrix must be calculated for each link. The matrices may then be concatenated, in the appropriate order, to obtain the transformation matrix which relates the pose of the disk in the disk frame, $\{D\}$ to the pose of the disk in the base frame of interest. Since the base frame $\{^A_0\}$ has been selected as the inertial reference frame, the locations of the bases of all other legs must be expressed with respect to $\{^A_0\}$ and incorporated into the calculations. The displacement equations for each leg may then be obtained, by inspection, from this transformation matrix.

After some algebra the following are obtained (note the right super–script is dropped, since all variables refer to the leg being solved for):

$$ K_x = l_1c_1 + (l_2 + r)c_{12} - d_3s_{12} \qquad (1) $$

$$ K_y = l_1s_1 + (l_2 + r)s_{12} + d_3c_{12} \qquad (2) $$

Where

$$ \begin{aligned} K_x &= x_D - l^{Ak}_{0x} \\ K_y &= y_D - l^{Ak}_{0y} \\ c_1 &= \cos({}^0\vartheta_1) \\ c_{12} &= \cos({}^0\vartheta_1 + {}^1\vartheta_2) \\ s_1 &= \sin({}^0\vartheta_1) \\ s_{12} &= \sin({}^0\vartheta_1 + {}^1\vartheta_2) \end{aligned} $$

For leg A, $K_x = x_D$ and $K_y = y_D$.

Once the displacement equations are known, the following procedure may be used to solve for the set of joint variables required to achieve a desired feasible pose. Equations (1) and (2) are squared and added. ${}^0\vartheta_1$ is eliminated using the identities:

$$ \begin{aligned} c_{12} &= c_1c_2 - s_1s_2 \\ s_{12} &= c_1s_2 + s_1c_2 \end{aligned} $$

The following equation in two variables, ${}^1\vartheta_2$ and ${}^2d_3$, is obtained:

$$ \begin{aligned} 0 = {} & 2l_1((l_2 + r)c_2 - d_3s_2) + l_2(2r + l_2) + l_1^2 + d_3^2 \\ & +r^2 - K_x^2 - K_y^2 \end{aligned} \qquad (3) $$

${}^2d_3$ can be determined because of special property 5) and the fact that the general plane motion is decomposable into pure translational and rotational components. In the algorithm, step 1 requires that the higher pair be locked. Hence, there is no change in ${}^2d_3$. Step 2 recovers the angular offset artificially caused by step 1. This is accomplished by fixed axis rotation of the disk about its centre. Step 3 is the actual pure rotational component of the motion. Again, it is pure rotation about the disk centre. Thus ${}^2d_3$ in each of steps 2 and 3 is given by:

$$ \text{Step 2:} \quad {}^2_T d_3 = {}^2d_{30} - r({}^0_T\vartheta_{20} - {}^0\vartheta_{20}) \qquad (4) $$

$$ \text{Step 3:} \quad {}^2d_3 = {}^2_T d_3 + r(\vartheta_D - \vartheta_{D0}) \qquad (5) $$

Determining the joint offsets by using the pure rolling constraint equations guarantees that the tangency condition is met since tangency is a necessary (although not sufficient) condition for pure rolling.

Equation (3) is now a function of just one unknown variable, ${}^1\vartheta_2$. Solving (3) for ${}^1\vartheta_2$ yields two solutions:

$$ {}^1\vartheta_2 = 2\arctan\left[\frac{K_1 \pm 2\sqrt{K_2}}{2K_3}\right] \qquad (6) $$

Where

$$ \begin{aligned} K_1 &= 4l_1d_3 \\ K_2 &= 2l_1^2(l_2^2 + d_3^2 + r^2) + 4l_2r(l_1^2 - d_3^2 + K_x^2 + K_y^2) \\ & \quad -2d_3^2(l_2^2 + r^2) + 2(K_x^2 + K_y^2)(l_1^2 + l_2^2 + d_3^2 + r^2) \\ & \quad -2K_x^2K_y^2 - 4l_2^3r - 6r^2l_2^2 - 4r^3l_2 - l_1^4 - l_2^4 \\ & \quad -d_3^4 - r^4 - K_x^4 - K_y^4 \\ K_3 &= l_1^2 + l_2^2 + d_3^2 + r^2 - K_x^2 - K_y^2 + 2l_2(r - l_1) \\ & \quad -2l_1r \end{aligned} $$

Solving for angles using tan^{-1} has an inherent ambiguity concerning the quadrant in which the angle lies. To remedy this, the two–argument inverse tangent function, $ATAN2(y, x)$ is used. It is defined by:

$$ ATAN2(y, x) \equiv $$

$$ \begin{aligned} tan^{-1}(y/x) &= \vartheta \text{ if } x > 0 \\ tan^{-1}(y/x) + \pi \text{ sgn}(y) &= \vartheta + \pi \text{ sgn}(y) \text{ if } x < 0 \\ tan^{-1}(\infty) \text{ sgn}(y) &= \frac{\pi}{2} \text{ sgn}(y) \text{ if } x = 0 \end{aligned} $$

Where:

$$ \text{sgn}(y) = \begin{cases} 1 & \text{if } y \geq 0 \\ -1 & \text{if } y < 0 \end{cases} $$

Thus, equation (6) becomes:

$$ {}^1\vartheta_2 = 2ATAN2\left[\frac{K_1 \pm 2\sqrt{K_2}}{2K_3}\right] \qquad (7) $$

For a general displacement, the four algorithm steps produce the following: From step 1 two values of ${}^1_T\vartheta_{20}$ are obtained from equation (3). Corresponding to each of these there is a unique value of ${}^0_T\vartheta_{10}$ that will satisfy both equations (1) and (2). From step 2, there is one value of ${}^2_T d_3$ obtained for each value of ${}^0_T\vartheta_{20}$ determined in step 1. Also, two values of each of ${}^1_T\vartheta_2$ and ${}^0_T\vartheta_1$ are obtained. Step 3 yields two values for ${}^2d_3$, one for each of the values of ${}^2_T d_3$ determined in step 2. For each value of ${}^2d_3$ there correspond two values for each of ${}^1\vartheta_2$ and ${}^0\vartheta_1$. These are the *elbow–up* and *elbow–down* solutions. Thus, for each leg there are up to four solutions. The solutions for each leg are uncoupled. Hence, for a manipulator with n legs, there are 4^n solutions, some of which may be complex conjugate pairs.

8. EXAMPLES

Fig. 3. The following three numerical examples deal with 1) pure rotation of the disk about its centre; 2) pure translation of the disk, no disk rotation; 3) combined translation and rotation. In all three examples,

the home position shown in Fig. 1 is the initial position. The fixed link parameters and initial conditions are as follows, where lengths are in "generic" units and angles are in degrees:

Fixed Link Parameters
$$\begin{array}{lllll} r & = & 4 & & \\ l_{0x}^{AB} & = & 10\sqrt{2} & & \\ l_{0y}^{AB} & = & 0 & & \\ l_1^A & = & l_1^B & = & 4 \\ l_2^A & = & l_2^B & = & 10 \end{array}$$

Initial Joint Parameters
$$\begin{array}{lllll} {}^2d_{30}^A & = & {}^2d_{30}^B & = & 0 \\ {}^0\vartheta_{10}^A & = & 135° & & \\ {}^0\vartheta_{10}^B & = & 45° & & \\ {}^1\vartheta_{20}^A & = & 270° & & \\ {}^1\vartheta_{20}^B & = & 90° & & \\ {}^0\vartheta_{20}^A & = & 45° & & \\ {}^0\vartheta_{20}^B & = & 135° & & \end{array}$$

Initial Pose Array
$$\begin{bmatrix} x_{D0} \\ y_{D0} \\ \vartheta_{D0} \end{bmatrix} = \begin{bmatrix} 5\sqrt{2} \\ 9\sqrt{2} \\ 0° \end{bmatrix}$$

Example 1

Pure rotation of the disk about its centre is the simplest motion for obtaining solutions. There are no intermediate joint parameters to calculate. As a result, a maximum of only four solutions may be expected.

In this example, the disk centre remains in its home position while it rotates through 15°. The desired pose array is:

$$\begin{bmatrix} x_D \\ y_D \\ \vartheta_D \end{bmatrix} = \begin{bmatrix} 5\sqrt{2} \\ 9\sqrt{2} \\ 15° \end{bmatrix}$$

The four solutions are given in Table 1 in the appendix and illustrated in

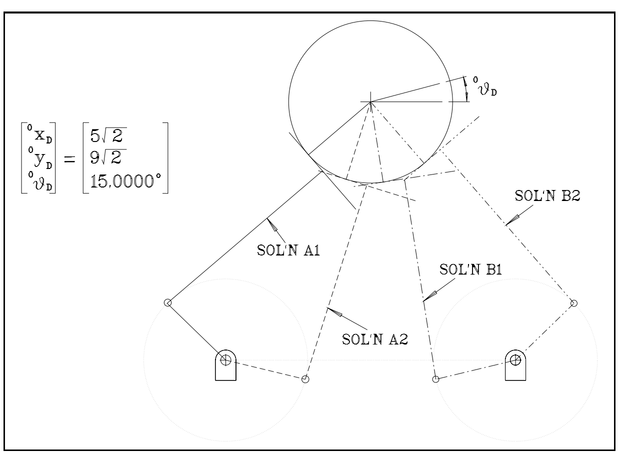

Figure 3. The solutions for pure rotation from Table 1.

Example 2

In this example, joint parameters are calculated for the case of pure translation of the disk. Despite the fact that no real rotation of the disk occurs, the algorithm requires the calculation of a set of intermediate joint variables. The desired pose array is:

$$\begin{bmatrix} x_D \\ y_D \\ \vartheta_D \end{bmatrix} = \begin{bmatrix} 2.0710 \\ 11.7280 \\ 0° \end{bmatrix}$$

The first four solutions are shown in Fig. 4. All sixteen solutions are given in Table 2 in the appendix.

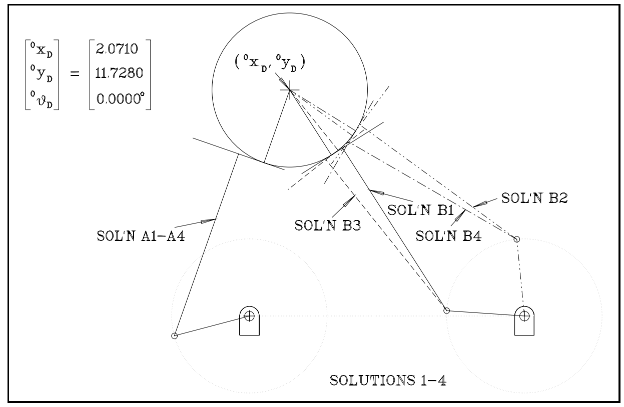

Figure 4. The first four solutions for pure translation from Table 2.

Example 3

The displacements of examples 1 and 2 are combined to give a general plane displacement. The desired pose array is:

$$\begin{bmatrix} x_D \\ y_D \\ \vartheta_D \end{bmatrix} = \begin{bmatrix} 2.0710 \\ 11.7280 \\ 15° \end{bmatrix}$$

Four of the sixteen solutions are illustrated in Fig. 5. All sixteen solutions are tabulated in Table 3 in the appendix.

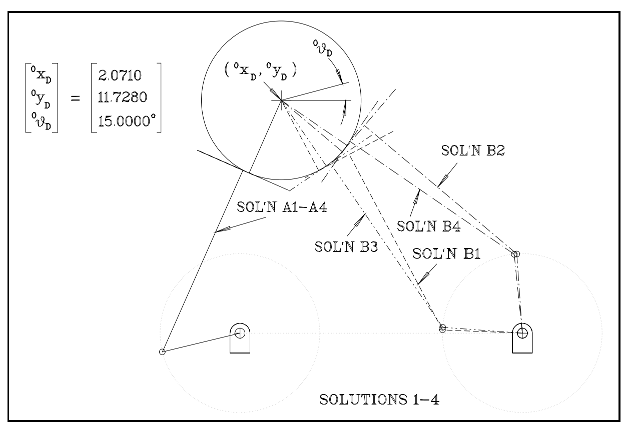

Figure 5. The first four solutions for general plane motion from Table 3.

9. CONCLUSIONS

In this paper, we have introduced an algorithm for solving the inverse kinematics problem of a class of planar parallel manipulators with holonomic higher pairs with $n\,2R$ legs. The seemingly complicated problem was reduced, at worst, to solution of quadratic equations. This reduction was achieved by "geometric thinking". That is, the kinematic geometry of the manipulator was analyzed, revealing properties which were in turn used to decompose the general inverse kinematics problem into simpler stages of pure translation and rotation.

However, the kinematic analysis merely begins with the inverse kinematics. The more complicated problem of the forward kinematics, which invites an excursion into the area of Grünwald's *kinematic mapping*, has yet to be addressed. Furthermore, issues of workspace singularities and assembly modes, isotropy, etc., are ripe for investigation. There are also ample interesting applications for this class of manipulator to warrant further study. For instance, a three legged version could be adapted as a 'universal' four–jaw chuck with a variable axis.

REFERENCES

[1] Angeles, J., 1988, "Rational Kinematics", Springer Tracts in Natural Philosophy, Springer-Verlag, New York.

[2] Argawal, S.K. & Pandravada, R., 1992, "Inverse Kinematic Solutions of a Rolling Disk Between Two Planar Manipulators", Robotics, Spatial Mechanisms, and Mechanical Systems, ASME, DE-Vol. 45, pp. 473-478.

[3] Argawal, S.K. & Pandravada, R., 1993, "Kinematics and Workspace of a Rolling Disk Between Planar Manipulators", Proc. Am. Control Conf., San Francisco, Cal., pp. 741-745.

[4] Biggs, N.L., 1989, "Discrete Mathematics", revised edition, Clarendon Press, Oxford.

[5] Bottema, O. & Roth, B., 1979, "Theoretical Kinematics", Dover Publications, Inc., New York.

[6] Cole, A., Hauser, J. & Sastry, S., 1988, "Kinematics and Control of Multifingered Hands with Rolling Contact", Proc. of IEEE Int. Conf. Rob. Aut., pp. 228-233.

[7] Coxeter, H.S.M., 1969, "Introduction to Geometry", second edition, John Wiley & Sons, Inc., Toronto.

[8] Craig, J.J., 1989, "Introduction to Robotics, Mechanics and Control", second edition, Addison-Wesley Publishing Co..

[9] Denavit, J. & Hartenberg, R.S., June 1955, "A Kinematic Notation for Lower-Pair Mechanisms Based on Matrices", J. of Applied Mechanics, pp. 215-221.

[10] Gosselin, C., 1988, "Kinematic Analysis, Optimization and Programming of Parallel Robotic Manipulators", Ph.D. thesis, Department of Mechanical Engineering, McGill University.

[11] Hartenberg, R.S., & Denavit, J., 1964, "Kinematic Synthesis of Linkages", McGraw-Hill, Book Co., New York.

[12] Hunt, K.H., 1978, "Kinematic Geometry of Mechanisms", Clarendon Press, Oxford.

[13] Mimura, N. & Funahashi, Y., 1992, "Kinematics of Planar Multifingered Robot Hand with Displacement of Contact Points", JSME International Journal, Series 3, Vol. 35, No. 3, pp. 462-469.

[14] O'Neill, B., 1966, "Elementary Differential Geometry", Academic Press, Inc..

[15] Saha, S.K., & Angeles, J., May 1989, "Kinematics and Dynamics of 3-wheeled 2-DOF AGV", Proc. of IEEE Int. Conf. Rob. Aut, Scottsdale, Ariz., pp. 1572-1577.

[16] Saha, S.K., & Angeles, J., March 1991, "Dynamics of Nonholonomic Mechanical Systems Using a Natural Orthogonal Compliment", J. of Applied Mechanics, ASME, Vol. 58, pp. 238-243.

[17] Salisbury, J.K. & Roth, B., March 1983, "Kinematic and Force Analysis of Articulated Mechanical Hands", J. of Mech., Trans., and Aut. in Design, ASME, Vol. 105, pp. 35-41.

[18] Sommerville, D.M.Y., 1934, "Analytical Geometry of Three Dimensions", Cambridge University Press, London.

[19] Yun, X., Kumar, V., Sarkar, N. & Paljug, E., May 1992, "Control of Multiple Arms with Rolling Constraints", Proc. of IEEE Int. Conf. Rob. Aut., Nice, France, pp. 2193-2198.

[20] Zsombor-Murrary, P., J. & Husty, M.L., June 1994, "Engineering Graphics, Computational Geometry and Geometric Thinking", Proc of ASEE Annual Conf., Edmonton, Alberta Vol. 1, pp. 437-443.

APPENDIX

Table 1.

Sol'n	1	2	3	4
${}^0\vartheta_1^A$ (deg)	135.5602	135.5602	-13.6694	-13.6694
${}^1\vartheta_2^A$ (deg)	265.1628	265.1628	-273.7183	-273.7183
${}^2d_3^A$	1.0472	1.0472	1.0472	1.0472
${}^0\vartheta_1^B$ (deg)	-166.3306	44.4398	-166.3306	44.4398
${}^1\vartheta_2^B$ (deg)	265.1628	-273.7183	265.1628	-273.7183
${}^2d_3^B$	1.0472	1.0472	1.0472	1.0472

Table 2.

Sol'n	1	2	3	4
${}^0\vartheta_1^A$ (deg)	-165.1389	-165.1389	-165.1389	-165.1389
${}^1\vartheta_2^A$ (deg)	235.8174	235.8174	235.8174	235.8174
${}^2d_3^A$	-1.3383	-1.3383	-1.3383	-1.3383
${}^0\vartheta_1^B$ (deg)	176.0545	95.5975	176.1665	95.4856
${}^1\vartheta_2^B$ (deg)	306.3702	-311.9312	312.2698	-305.7674
${}^2d_3^B$	0.6799	0.6799	-0.7953	-0.7953
Sol'n	5	6	7	8
${}^0\vartheta_1^A$ (deg)	-34.8899	-34.8899	-34.8899	-34.8899
${}^1\vartheta_2^A$ (deg)	-224.5344	-224.5344	-224.5344	-224.5344
${}^2d_3^A$	-1.3383	-1.3383	-1.3383	-1.3383
${}^0\vartheta_1^B$ (deg)	176.0545	95.5975	176.1665	95.4856
${}^1\vartheta_2^B$ (deg)	306.3702	-311.9312	312.2698	-305.7674
${}^2d_3^B$	0.6799	0.6799	-0.7953	-0.7953
Sol'n	9	10	11	12
${}^0\vartheta_1^A$ (deg)	-158.0567	-158.0567	-158.0567	-158.0567
${}^1\vartheta_2^A$ (deg)	238.4847	238.4847	238.4847	238.4847
${}^2d_3^A$	-3.5019	-3.5019	-3.5019	-3.5019
${}^0\vartheta_1^B$ (deg)	176.0545	95.5975	176.1665	95.4856
${}^1\vartheta_2^B$ (deg)	306.3702	-311.9312	312.2698	-305.7674
${}^2d_3^B$	0.6799	0.6799	-0.7953	-0.7953
Sol'n	13	14	15	16
${}^0\vartheta_1^A$ (deg)	-41.9721	-41.9721	-41.9721	-41.9721
${}^1\vartheta_2^A$ (deg)	-210.3971	-210.3971	-210.3971	-210.3971
${}^2d_3^A$	-3.5019	-3.5019	-3.5019	-3.5019
${}^0\vartheta_1^B$ (deg)	176.0545	95.5975	176.1665	95.4856
${}^1\vartheta_2^B$ (deg)	306.3702	-311.9312	312.2698	-305.7674
${}^2d_3^B$	0.6799	0.6799	-0.7953	-0.7953

Table 3.

Sol'n	1	2	3	4
${}^0\vartheta_1^A$ (deg)	-166.3263	-166.3263	-166.3263	-166.3263
${}^1\vartheta_2^A$ (deg)	232.5227	232.5227	232.5227	232.5227
${}^2d_3^A$	-0.3358	-0.3358	-0.3358	-0.3358
${}^0\vartheta_1^B$ (deg)	177.6881	93.9640	175.7910	95.8611
${}^1\vartheta_2^B$ (deg)	300.1970	-314.2627	308.4310	-310.4928
${}^2d_3^B$	1.7271	1.7271	0.2519	0.2519
Sol'n	5	6	7	8
${}^0\vartheta_1^A$ (deg)	-33.7025	-33.7025	-33.7025	-33.7025
${}^1\vartheta_2^A$ (deg)	-229.7750	-229.7750	-229.7750	-229.7750
${}^2d_3^A$	-0.3358	-0.3358	-0.3358	-0.3358
${}^0\vartheta_1^B$ (deg)	176.0545	95.5975	175.7910	95.8611
${}^1\vartheta_2^B$ (deg)	300.1970	-314.2627	308.4310	-310.4928
${}^2d_3^B$	1.7271	1.7271	0.2519	0.2519
Sol'n	9	10	11	12
${}^0\vartheta_1^A$ (deg)	-162.3804	-162.3804	-162.3804	-162.3804
${}^1\vartheta_2^A$ (deg)	237.8740	237.8740	237.8740	237.8740
${}^2d_3^A$	-2.4548	-2.4548	-2.4548	-2.4548
${}^0\vartheta_1^B$ (deg)	176.0545	95.5975	175.7910	95.8611
${}^1\vartheta_2^B$ (deg)	300.1970	-314.2627	308.4310	-310.4928
${}^2d_3^B$	1.7271	1.7271	0.2519	0.2519
Sol'n	13	14	15	16
${}^0\vartheta_1^A$ (deg)	-37.6483	-37.6483	-37.6483	-37.6483
${}^1\vartheta_2^A$ (deg)	-217.9837	-217.9837	-217.9837	-217.9837
${}^2d_3^A$	-2.4548	-2.4548	-2.4548	-2.4548
${}^0\vartheta_1^B$ (deg)	176.0545	95.5975	175.7910	95.8611
${}^1\vartheta_2^B$ (deg)	300.1970	-314.2627	308.4310	-310.4928
${}^2d_3^B$	1.7271	1.7271	0.2519	0.2519